OPEN ACCESS

Saudi Journal of Medical and Pharmaceutical Sciences
Abbreviated Key Title: Saudi J Med Pharm Sci
ISSN 2413-4929 (Print) | ISSN 2413-4910 (Online)
Scholars Middle East Publishers, Dubai, United Arab Emirates
Journal homepage: https://saudijournals.com

Original Research Article **Radiology**

ADC as a Correlative Marker of ^{18}F-Fdopa Pet-Defined Metabolic Activity in Newly Diagnosed Glioma: A Retrospective Imaging-Correlation and Diagnostic Performance Analysis

Imad Kh. Resen[1]*, Zamazam Hussein Shummar[1], Saradiq Mudhafar Jebur[2]

[1]Assistant Lecturer, Radiology Department, Dijlah University College, Baghdad, Iraq
[2]Radiology Department, Dijlah University College, Baghdad, Iraq

DOI: https://doi.org/10.36348/sjmps.2026.v12i08.003 | **Received:** 14.06.2026 | **Accepted:** 03.08.2026 | **Published:** 08.08.2026

***Corresponding author:** Imad Kh. Resen
Assistant Lecturer, Radiology Department, Dijlah University College, Baghdad, Iraq

Abstract

Objective: To evaluate the association and discriminatory performance of diffusion MRI-derived apparent diffusion coefficient (ADC) values for ^{18}F-FDOPA PET-defined metabolic activity in newly diagnosed glioma. ***Methods:*** This was a retrospective study of 87 treatment-naïve adults, who were initially evaluated for newly diagnosed or radiologically suspected glioma at Baghdad Teaching Hospital, Medical City, Baghdad from January 2026 to July 2026. Pretreatment diffusion MRI and ^{18}F-FDOPA PET/CT results were evaluated. PET activity was determined a priori as TBRmax ≥1.60 as an approximated operational application of PET RANO 1.0. The mean ADC was compared across PET groups, associated with SUVmax and TBRmax and assessed by ROC analysis. WHO grade analyses were done in 80 individuals with histological confirmation. ***Results:*** Forty-six tumors were PET-active and 41 were PET-inactive. Mean ADC was lower in PET-active tumors (1.04 ± 0.24 vs 1.16 ± 0.23 ×10^{-3} mm²/s; p=0.029), whereas SUVmax was higher (3.73 ± 0.98 vs 2.06 ± 0.45; p<0.001). ADC correlated inversely with TBRmax (Spearman rho=−0.32; p=0.003) and SUVmax (rho=−0.29; p=0.006). The AUC was 0.62 (95% CI, 0.50–0.74). At ADC ≤1.20 ×10^{-3} mm²/s, sensitivity was 84.8%, specificity 41.5%, and accuracy 64.4%. ***Conclusion:*** ADC was moderately inversely correlated with 18F-FDOPA uptake but was poor in discriminative ability alone. The lower bound of the AUC confidence interval was near chance performance. The cutoff from this cohort is experimental and should not be used for guiding clinical choices without external confirmation.

Keywords: Glioma; diffusion-weighted imaging; apparent diffusion coefficient; ^{18}F- FDOPA; amino acid PET; PET/MRI; ROC analysis; neuro-oncology.

INTRODUCTION

Gliomas remain challenging tumors to evaluate by imaging because their growth is infiltrative, their biological behavior is heterogeneous, and the visible MRI abnormality does not always correspond to the most active tumor component. Conventional MRI remains central to tumor detection, anatomical delineation, surgical planning, biopsy guidance, radiotherapy planning, and post-treatment surveillance. But there are constraints to traditional morphological evaluation. Structural changes such as contrast enhancement, FLAIR signal abnormalities, edema, necrosis and mass effect do not reliably indicate areas of greatest cellular, molecular or metabolic activity. This mismatch has led to the increasing use of physiologic and metabolic imaging biomarkers in neuro-oncology [4,6,12,13]. Previous voxel-wise and patient-wise comparisons between ^{18}F-FDOPA PET and physiologic MRI parameters demonstrated measurable correlations, while also indicating that PET and MRI capture partly different aspects of glioma biology [1].

Diffusion-weighted imaging is particularly attractive because it is widely available, does not require an exogenous radioactive tracer, and is already incorporated into most brain tumor MRI protocols. The apparent diffusion coefficient is often used as an indirect index of tissue cellularity, with lower ADC values typically indicating more limited extracellular water mobility in highly cellular tumour tissue. But this is not a one-to-one correlation. Quantification of ADC values

can be influenced by necrosis, cystic degeneration, hemorrhage, vasogenic edema, partial-volume averaging, scanner-related variability, ROI placement, and intratumoral heterogeneity. Quantitative MRI studies combined with amino acid PET and stereotactic tissue validation confirm the biological importance of MRI-derived microstructural biomarkers, but also demonstrate that no single quantitative MRI measure can properly define a heterogeneous glioma [2,11]. More broadly, multimodal PET/MRI studies suggest that diffusion and metabolic imaging may overlap in aggressive tumor regions, yet they remain biologically non-equivalent measurements [1,6].

Amino acid PET, including ^{18}F-FDOPA PET, assesses another aspect of tumour behaviour, mainly amino acid transport and metabolically active tumour tissue. Amino acid PET can be used in neuro-oncologic practice to delineate lesions, to target biopsies, to plan radiotherapy, to grade tumours, to monitor recurrence and to differentiate live tumour from treatment-related alteration. [3,4,12,13]. This role becomes more important in clinically uncertain settings, particularly after surgery or radiotherapy, where enhancement, radiation injury, pseudoprogression, and recurrent tumor may overlap on conventional MRI [3,9,10]. For the neuroradiologist, amino acid PET/MRI is not simply another picture collection. It gives supplementary biological information which may demonstrate active tumour beyond obvious anatomical limits [4,6].

Recent evidence indicates that combining amino acid PET with MRI improves identification of malignant and metabolically active regions in adult glioma [5]. Hybrid PET/MRI also enables integrated assessment of anatomy, diffusion, perfusion, metabolism, and imaging features related to tumor phenotype [6]. Other amino acid tracers, including anti-3-[^{18}F] FACBC and ^{18}F-FET, have shown diagnostic value in glioma evaluation, although their availability, uptake behavior, and clinical performance vary between institutions and tracers [7,9,11,12]. For ^{18}F-FDOPA specifically, static and dynamic PET techniques have been useful for glioma characterisation, grading and identification of aggressive tumour behaviour beyond standard morphological imaging [8,13]. PET RANO 1.0 has provided a structured framework for amino acid PET interpretation in diffuse gliomas [16], while recent methodological application to ^{18}F-FDOPA has supported more consistent lesion-to-background assessment despite the difficulty created by physiological striatal uptake [17].

However, despite these advances, amino acid PET is still not widely available in many centres, while diffusion MRI is routinely available. ADC should not be regarded a surrogate for amino acid PET, as diffusion restriction and amino acid absorption are distinct biological processes. It could still be a correlated signal in the wider imaging assessment. The present study therefore examined the association between ADC and ^{18}F-FDOPA PET-defined metabolic activity in patients undergoing initial assessment for glioma. The aims were to quantify this association, assess the discriminatory performance of ADC, and determine how much biological and imaging overlap limits its classification value.

MATERIALS AND METHODS

Study Design, Setting, and Dataset

We conducted this retrospective imaging-correlation and diagnostic performance study at Baghdad Teaching Hospital, Medical City, Baghdad, Iraq. We reviewed every eligible adult case available between January and July 2026 rather than selecting a random sample. In total, 87 patients met the study criteria.

Our investigation was limited to participants being assessed for a new or radiologically suspected glioblastoma. Inclusion criteria were pre-treatment diffusion-weighted MRI with ADC maps for each subject, ^{18}F-FDOPA PET/CT adequate clinical and imaging data to determine all pre-specified research factors. Patients were eliminated if they did not have paired MRI and PET exams, if image quality was not optimal for analysis, if ADC or PET measures could not be collected, or if they had already started tumor-directed therapy before to imaging. All MRI and PET scans included in this research were obtained prior to surgery, radiation, chemotherapy or any other tumor-directed therapy. The retrospective design of the study did not allow us reliably extract the precise gap between MRI and PET for all patients.

Our primary objective was to evaluate the relationship between diffusion-derived ADC measurements and metabolic activity defined by ^{18}F-FDOPA PET. Therefore, PET metabolic state was used as a reference imaging result. It was not meant to substitute histopathology or integrated histomolecular diagnosis. Thus, the diagnostic performance presented here is an assessment of ADC to distinguish a pre-specified PET imaging goal rather than to predict histological grade, molecular subtype or biological viability. The variables collected for analysis included integrated histomolecular diagnosis, WHO grade, mean ADC, SUVmax, TBRmax, contrast enhancement, necrosis or cystic change, FLAIR signal abnormality or edema, visually assessed diffusion restriction, and susceptibility abnormalities identified on SWI or T2*-weighted imaging.

Histopathological confirmation was available in 80 of the 87 patients (92.0%). The remaining seven patients were retained in analyses that used PET-defined metabolic activity as the reference imaging endpoint but were omitted from analysis of WHO grade or histo-molecular categorisation. This was done since the current categorisation of glioma is based on a combination of histology and molecular data, as outlined

in the 2021 WHO Classification of Tumors of the Central Nervous System [14].

MRI Acquisition

Brain MRI examinations were performed on a 1.5-T Philips MRI system using a clinical adult brain tumor protocol. The available protocol included axial T1-weighted imaging, axial T2-weighted imaging, axial fluid-attenuated inversion recovery (FLAIR), diffusion-weighted imaging with ADC map generation, and susceptibility-sensitive imaging using either SWI or T2*-weighted gradient-echo imaging. Post-contrast three-dimensional T1-weighted imaging was obtained after administration of a gadolinium-based contrast agent when clinically indicated.

Diffusion-weighted imaging was performed using single-shot echo-planar imaging with at least 2 b-values, most often b=0 and b=1000 s/mm². 3 mm was the reconstructed slice thickness and ADC values were given in $\times 10^{-3}$ mm²/s. No explicit ADC harmonisation or cross-scanner normalisation was applied.

Post-contrast T1-weighted images were evaluated for solid or ring enhancement and non-enhancing necrotic or cystic components. FLAIR images were assessed for non-enhancing infiltrative tumour signal and surrounding parenchymal signal abnormalities or oedema. SWI or T2*-weighted images were evaluated for intratumoral haemorrhage, mineralisation or calcification-related susceptibility, and other localised susceptibility changes.

ADC Measurement and Image Interpretation

The primary quantitative MRI variable was the mean ADC. Three circular sections of interest about 2 mm in diameter were manually put in distinct typical regions of visibly solid tumour tissue. The three data were averaged to get the patient-level mean ADC that was utilized in the analysis.

In enhancing tumors, ROIs were placed within solid enhancing components. In non-enhancing tumors, ROIs were positioned in the most suspicious solid FLAIR-hyperintense component, guided by lesion morphology and diffusion characteristics. Necrotic or cystic areas, macroscopic hemorrhage, suspected calcification, large vessels, lesion margins, adjacent cerebrospinal fluid, normal brain tissue, and obvious artifacts were avoided.

ADC measurement responsibilities were shared among four radiologists using the same predefined placement rules. The cases were split among the reading crew with each read adding a single final set of three ROI measurements to the data set. Reader-level identities and duplicate independent measurements were not kept and a formal interobserver agreement analysis could not be performed. In the retrospective collection, formal blinding between the MRI and PET evaluations was not documented. Visual diffusion limitation was independently recorded as high signal on high-b-value DWI with associated low signal on the ADC map.

^{18}F-FDOPA PET/CT Acquisition and Quantitative Analysis

^{18}F-FDOPA PET/CT examinations were performed using the routine static brain PET/CT workflow at Baghdad Teaching Hospital, Medical City, Baghdad. Patients received ^{18}F-FDOPA intravenously, followed by a predefined clinical uptake interval before static brain PET acquisition. A low-dose non-contrast CT scan was obtained for attenuation correction and anatomical localization. PET reconstruction incorporated corrections for attenuation, scatter, random coincidences, and radioactive decay.

Complete case-level documentation of injected activity, exact uptake interval, scanner model, carbidopa premedication status, and reconstruction settings could not be retrieved consistently from the retrospective archive. These values were not imputed from published protocols or treated as study variables.

The principal quantitative PET variables were SUVmax and TBRmax. SUVmax was defined as the highest measured uptake within the most metabolically active tumor region. TBRmax was calculated by dividing tumor SUVmax by mean uptake in contralateral normal-appearing cortical or subcortical tissue. Background regions avoided tumor infiltration, FLAIR abnormality or edema, hemorrhage, infarction, and deep gray nuclei because physiological ^{18}F-FDOPA uptake is high within the striatum.

One was in the thalamic/basal ganglia area. In this scenario, the background activity was taken from the contralateral normal-appearing cortical or subcortical tissue outside the deep grey nuclei, in line with the concepts of organised lesion to background evaluation. [16,17].

PET Reference Outcome

The standard scan result was metabolic activity as described by PET. When the uptake in the same part of the body achieved a certain TBRmax level of 1.60, the tumour was considered PET-active. A visual check was done to make sure that the rise was due to the tumour and not to normal striatal activity, mistaken registration, or something else that wasn't the tumour.

The threshold was specified before ADC ROC analysis and was therefore independent of the ADC-derived cutoff. PET RANO 1.0 uses uptake of at least 1.6 times mean background activity for amino acid PET positivity [16], and a later methodological study applied this rule to ^{18}F-FDOPA PET [16]. At this point in time, before treatment, this was not a direct validation of a diagnostic cutoff but rather an extrapolated operational use of a response-oriented framework. There isn't a single biological or histopathological standard for 1.60 because FDOPA-specific histological confirmation isn't

always the same and some studies have used higher limits.

The study used patient-level binary PET classification and did not constitute a full volumetric PET RANO treatment-response assessment.

Imaging Variables and Dataset Structure

We looked at mean ADC, visual diffusion restriction, contrast enhancement, necrosis or cystic change, FLAIR abnormality or oedema, and susceptibility abnormality on SWI or T2*-weighted images. These were the main MRI factors. TBRmax and SUVmax were the PET factors. Using a set rule, PET activity was coded as either active or inactive.

Since PET activity was directly linked to TBRmax, differences in TBRmax between groups that had PET activity and groups that did not had PET activity were only reported as details and not as separate comparisons for inference. When pathological proof was provided, the combined histomolecular diagnosis and WHO grade were looked at.

Statistical Analysis

Continuous variables were summarised as mean ± standard deviation for normal distribution and median with interquartile range for non-normal distribution. Categorical variables were frequency and percentage. Normality was assessed using the Shapiro–Wilk test and histogram and quantile–quantile plot inspection.

Mean ADC was compared between PET-active and PET-inactive groups using Welch's independent-samples t-test. SUVmax was compared using the Mann–Whitney U test due of its non-normal distribution. Due to PET group definition, TBRmax was reported descriptively by PET status without an independent significance test. The chi-square or Fisher's exact test was used to compare categorical MRI variables as exploratory secondary comparisons.

ROC analysis assessed PET-defined activity ADC discrimination. Youden index-selected ADC threshold was cohort-derived. With 95% confidence intervals, AUC, sensitivity, specificity, positive and negative predictive values, likelihood ratios, and accuracy were determined. The SPSS nonparametric asymptotic approach calculated the AUC confidence interval. Binomial diagnostic proportion intervals were calculated using the Wilson method, and logarithmic likelihood-ratio intervals were estimated.

Spearman's rank correlation coefficient examined SUVmax and TBRmax-ADC relationships. ONLY histopathologically confirmed tumours were used to compare WHO grades 3 and 4 as a high-grade subgroup to grade 2. Secondary and exploratory categorical MRI and grade-based comparisons did not need multiplicity correction. P-values were hypothesis-generating, not confirming.

For the primary analysis, all tests were two-sided and $p<0.05$ was deemed significant. IBM SPSS Statistics (2023 version; IBM Corp., Armonk, NY, USA) was used for analyses. No sample-size calculation was done; all eligible records from the predefined retrospective period were sampled. We excluded affected cases from pathology-dependent analyses and did not impute missing pathological data. The final analytic dataset had no uncertain ADC or PET classifications. STARD 2015 guided reporting [15]. Diagnostic estimates may be optimistic because the ADC threshold was chosen and tested in the same cohort.

Ethical Considerations

The study protocol was reviewed and approved by the Medical Scientific Committee of Baghdad Teaching Hospital, Medical City, Baghdad, Iraq (approval no. 2-5543; 20 July 2026). The approval covered retrospective review of routine-care records generated during the study period.

Because this was a retrospective study using anonymized clinical, imaging, PET, and pathological records obtained during routine care, the requirement for individual informed consent was waived by the approving committee. Direct patient identifiers were removed before analysis. The study followed institutional ethical requirements and the Declaration of Helsinki.

RESULTS

Patient Flow and Baseline Characteristics

The final analytic cohort included 87 adults with newly diagnosed glioma (Figure 1). Based on the predefined ^{18}F-FDOPA PET criterion, 46 patients were classified as PET-active (52.9%) and 41 as PET-inactive (47.1%).

Histopathological confirmation was available for 80 patients (92.0%). Of these, 32 had WHO grade 2, 20 grade 3, and 28 grade 4 glioma. Seven patients without histopathological confirmation were excluded from WHO grade-based and histomolecular subgroup analyses. Mean age was 48.5 ± 15.0 years (range, 19–82 years). The cohort included 51 women (58.6%) and 36 men (41.4%) (Table 1).

Table 1: Baseline demographic and clinical characteristics

Variable	Value
Total patients	87
Age, years	48.5 ± 15.0

Variable	Value
Age range, years	19–82
Male sex	36 (41.4%)
Female sex	51 (58.6%)
PET-active glioma	46 (52.9%)
PET-inactive glioma	41 (47.1%)
Histopathology available	80 (92.0%)
Histopathology unavailable	7 (8.0%)
WHO grade 2	32
WHO grade 3	20
WHO grade 4	28
WHO grades 3–4 combined	48

Values are mean ± standard deviation or number (%), as appropriate. WHO grade categories include histopathologically confirmed cases only.

Tumor Location

The insular or deep cerebral regions and the parietal lobe were the most common places for dominant tumours, with 20 patients (23.0% of all patients) having them. In 18 of the cases, there were temporal tumours (20.7%), followed by frontal tumors in 14 (16.1%) (Table 2).

Table 2: Distribution of dominant tumor location

Tumor location	Number (%)
Insular/deep cerebral region	20 (23.0%)
Parietal lobe	20 (23.0%)
Temporal lobe	18 (20.7%)
Frontal lobe	14 (16.1%)
Corpus callosum	8 (9.2%)
Multifocal	6 (6.9%)
Thalamic/basal ganglia	1 (1.1%)

Conventional MRI and Diffusion Findings

PET-active tumours showed more frequent contrast enhancement, necrosis or cystic change, visual diffusion limitation, FLAIR oedema, and susceptibility anomalies (Table 3). These category comparisons were exploratory and secondary. Mean ADC of PET-active group was less than PET-inactive group (1.04 ± 0.24 vs 1.16 ± 0.23 $\times 10^{-3}$ mm²/s; p=0.029). Despite the statistically significant difference, substantial overlap was present between distributions (Figure 3).

Table 3: MRI findings according to PET-defined metabolic status

MRI variable	PET-active (n=46)	PET-inactive (n=41)	p-value
Contrast enhancement	34 (73.9%)	10 (24.4%)	<0.001
Necrosis or cystic change	21 (45.7%)	1 (2.4%)	<0.001
Visual diffusion restriction	28 (60.9%)	10 (24.4%)	0.001
FLAIR edema	32 (69.6%)	15 (36.6%)	0.003
SWI or T2* abnormality	22 (47.8%)	9 (22.0%)	0.014
Mean ADC, $\times 10^{-3}$ mm²/s	1.04 ± 0.24	1.16 ± 0.23	0.029

ADC was compared using Welch's independent-samples t-test. Categorical variables were compared using the chi-square test or Fisher's exact test, as appropriate. Categorical MRI comparisons were exploratory, and no formal multiplicity adjustment was applied.

^{18}F-FDOPA PET/CT Findings

Tumor SUVmax was higher in PET-active than PET-inactive tumors (3.73 ± 0.98 vs 2.06 ± 0.45; p<0.001). Mean TBRmax was 2.21 ± 0.42 in PET-active tumors and 1.29 ± 0.19 in PET-inactive tumors. TBRmax was reported descriptively without independent inferential testing because PET status was defined directly by TBRmax (Table 4).

Table 4: Quantitative PET parameters according to PET-defined metabolic status

PET parameter	PET-active (n=46)	PET-inactive (n=41)	p-value
Tumor SUVmax	3.73 ± 0.98	2.06 ± 0.45	<0.001
TBRmax	2.21 ± 0.42	1.29 ± 0.19	Not tested*

**TBRmax was used to define PET metabolic status; an independent between-group significance test would therefore be circular.*

Relationship Between ADC and PET-Derived Uptake

ADC showed a modest inverse association with TBRmax (Spearman rho=−0.32; p=0.003) and SUVmax (rho=−0.29; p=0.006) (Table 5 and Figure 4).

Table 5: Correlation between ADC and PET-derived uptake parameters

Correlation	Spearman rho	p-value	Interpretation
ADC vs TBRmax	−0.32	0.003	Modest inverse association
ADC vs SUVmax	−0.29	0.006	Modest inverse association

Diagnostic Performance of ADC

ROC analysis revealed restricted differentiation of PET-defined metabolic activity by ADC (Figure 2). The AUC measured 0.62 (95% CI, 0.50–0.74). At the cohort-established Youden criterion of ADC ≤1.20 ×10⁻³ mm²/s, there were 39 true-positive patients, 24 false-positive patients, 17 true-negative patients, and seven false-negative patients. Sensitivity was recorded at 84.8% (95% CI, 71.8–92.4%), specificity at 41.5% (95% CI, 27.8–56.6%), positive predictive value at 61.9% (95% CI, 49.6–72.9%), negative predictive value at 70.8% (95% CI, 50.8–85.1%), and total accuracy at 64.4% (95% CI, 53.9–73.6%). The positive likelihood ratio was 1.45 (95% CI, 1.09–1.93), whereas the negative likelihood ratio was 0.37 (95% CI, 0.17–0.80) (refer to Table 6 and Figure 5).

A subsequent, more stringent criterion of ADC ≤0.98 ×10⁻³ mm²/s enhanced specificity to 78.0% while diminishing sensitivity to 37.0%; the overall accuracy was recorded at 56.3%. This secondary analysis was investigative.

Table 6: Diagnostic performance of ADC for PET-defined metabolic activity

Diagnostic metric	Result
AUC	0.62 (95% CI, 0.50–0.74)
Cohort-derived ADC threshold	≤1.20 ×10⁻³ mm²/s
True-positive	39
False-positive	24
True-negative	17
False-negative	7
Sensitivity	84.8% (95% CI, 71.8–92.4%)
Specificity	41.5% (95% CI, 27.8–56.6%)
Positive predictive value	61.9% (95% CI, 49.6–72.9%)
Negative predictive value	70.8% (95% CI, 50.8–85.1%)
Positive likelihood ratio	1.45 (95% CI, 1.09–1.93)
Negative likelihood ratio	0.37 (95% CI, 0.17–0.80)
Overall accuracy	64.4% (95% CI, 53.9–73.6%)

The threshold was derived and evaluated in the same cohort and represents apparent in-sample performance; it has not been externally validated.

Imaging Pattern According to WHO Grade

Among the 80 histopathologically confirmed tumors, PET activity was present in eight of 32 WHO grade 2 tumors (25.0%), 11 of 20 grade 3 tumors (55.0%), and 25 of 28 grade 4 tumors (89.3%) (Figure 6). For inferential analysis, grades 3 and 4 were combined as a high-grade subgroup: PET activity was present in 36 of 48 high-grade tumors (75.0%) compared with eight of 32 grade 2 tumors (25.0%; p<0.001).

Mean ADC was lower in the combined high-grade subgroup than in grade 2 tumors (0.97 ± 0.19 vs 1.28 ± 0.21 ×10⁻³ mm²/s; p<0.001). SUVmax and TBRmax were higher in high-grade tumors (3.50 ± 1.14 and 2.08 ± 0.55, respectively) than in grade 2 tumors (2.24 ± 0.69 and 1.40 ± 0.28; both p<0.001). Grade 3 and grade 4 values are presented descriptively in Table 7.

Table 7: Quantitative imaging pattern according to WHO grade

Parameter	WHO grade 2 (n=32)	WHO grade 3 (n=20)	WHO grade 4 (n=28)	Grades 3–4 combined (n=48)	p-value*
ADC, ×10⁻³ mm²/s	1.28 ± 0.21	1.03 ± 0.17	0.93 ± 0.19	0.97 ± 0.19	<0.001
SUVmax	2.24 ± 0.69	3.01 ± 0.86	3.85 ± 1.20	3.50 ± 1.14	<0.001
TBRmax	1.40 ± 0.28	1.82 ± 0.51	2.27 ± 0.50	2.08 ± 0.55	<0.001
PET-active	8/32 (25.0%)	11/20 (55.0%)	25/28 (89.3%)	36/48 (75.0%)	<0.001

**Inferential p-values compare WHO grade 2 with the combined grade 3–4 subgroup. Grade 3 and grade 4 columns are descriptive.*

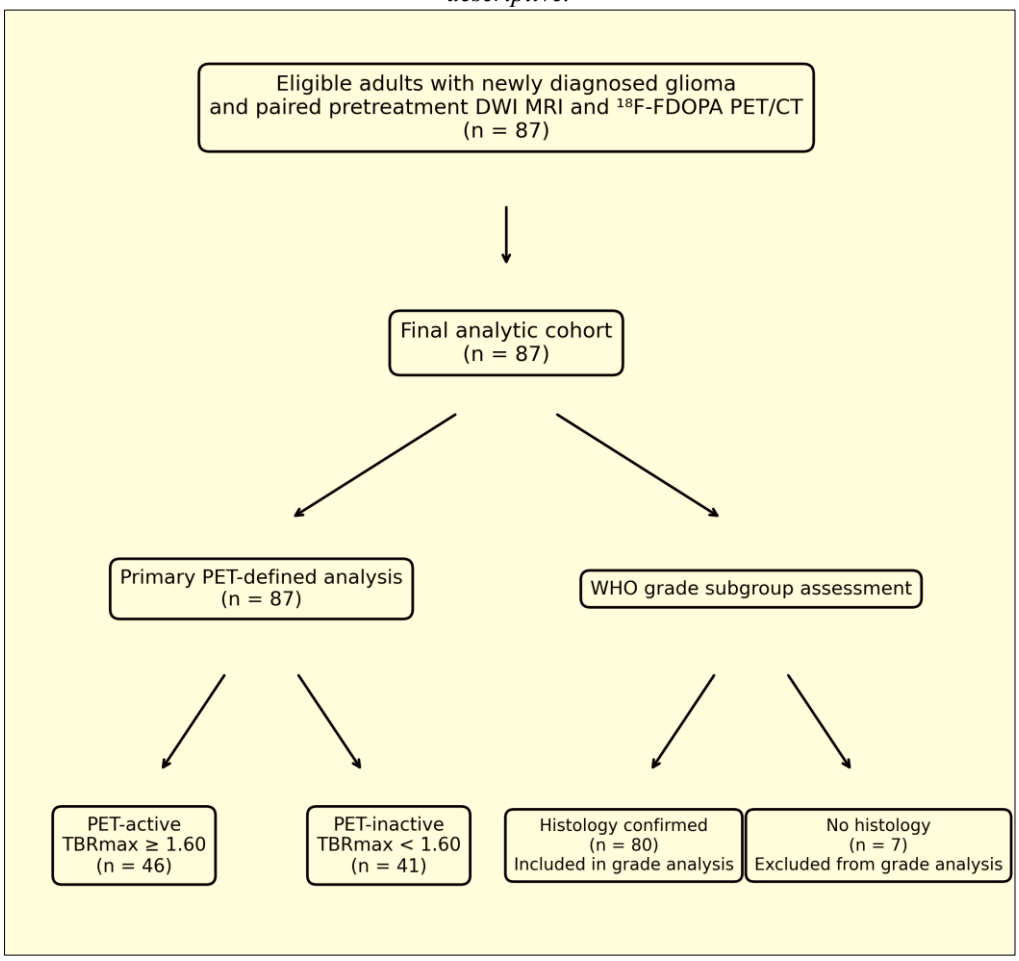

Figure 1: Patient flow diagram for PET-defined and WHO grade-based analyses

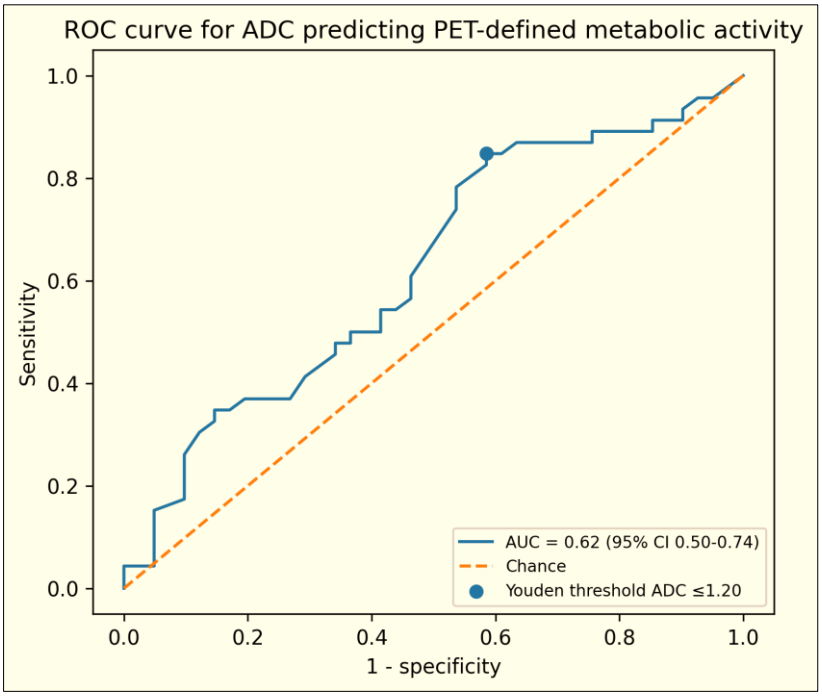

Figure 2: Receiver operating characteristic curve for ADC discrimination of PET-defined metabolic activity. AUC=0.62 (95% CI, 0.50–0.74)

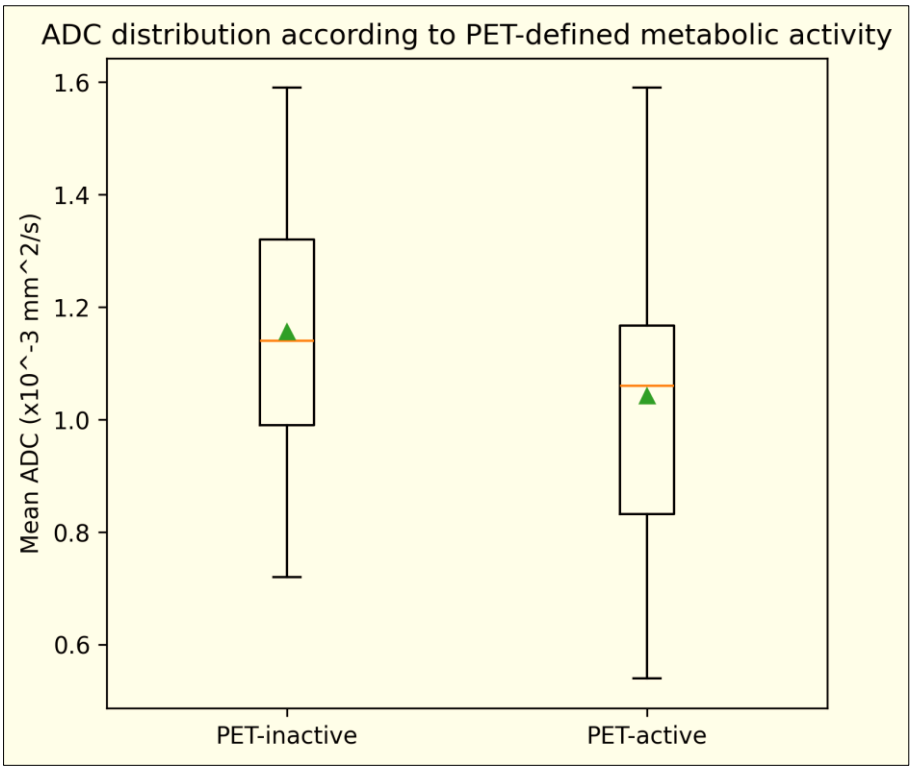

Figure 3: Distribution and overlap of ADC values in PET-active and PET-inactive gliomas. Triangles indicate group means

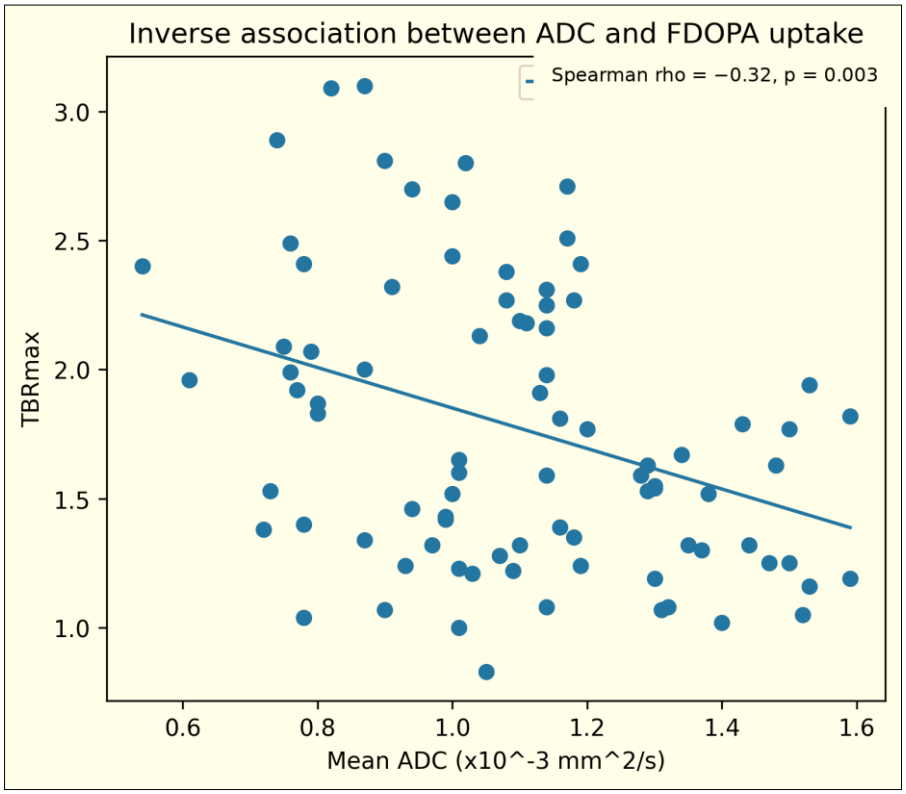

Figure 4: Scatter plot showing the modest inverse association between ADC and TBRmax (Spearman rho=−0.32; p=0.003)

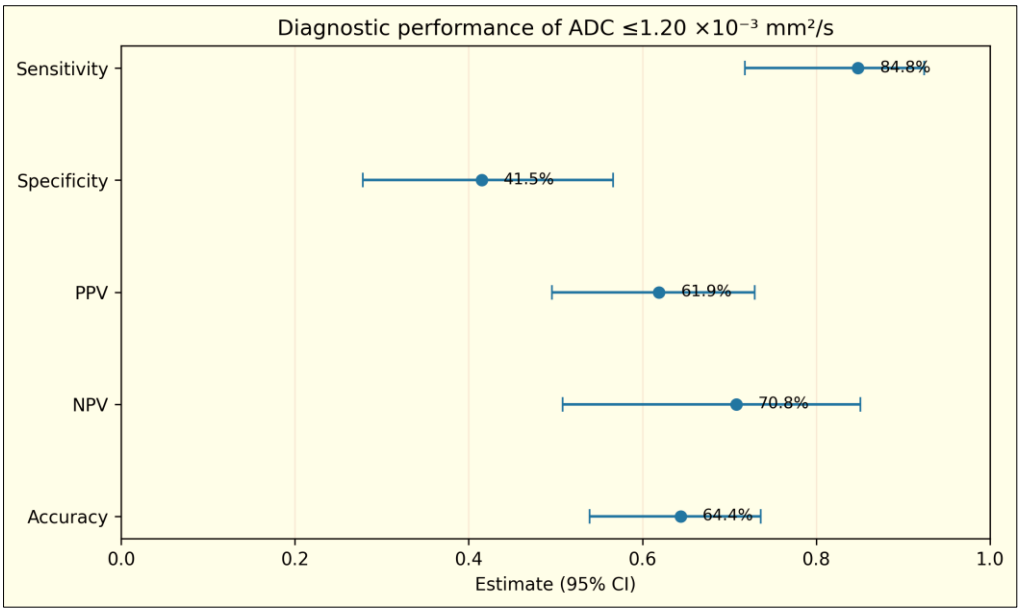

Figure 5: Point estimates and 95% confidence intervals for diagnostic performance at the cohort-derived ADC threshold of ≤1.20 ×10⁻³ mm²/s

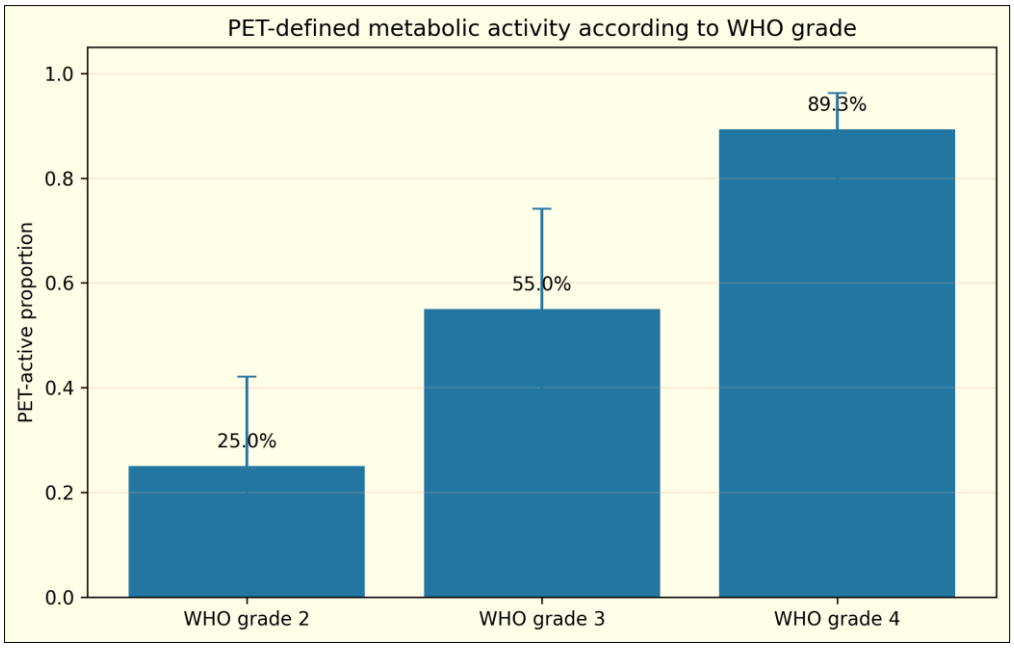

Figure 6: PET-active proportion by WHO grade. Error bars show Wilson 95% confidence intervals

DISCUSSION

This retrospective pretreatment glioma cohort showed a statistically significant relationship between ADC and ^{18}F-FDOPA PET-defined metabolic activity, although the clinical implications are somewhat limited. PET-active tumours showed a lower mean ADC and a higher SUVmax compared to PET-inactive tumours. The relationships between ADC and TBRmax as well as SUVmax were inversely related but only to a modest degree. Additionally, the ability of ADC to distinguish was somewhat limited, reflected by an AUC of 0.62. The main takeaway was not about finding a difference, but rather how much the tumours overlapped. ADC and ^{18}F-FDOPA uptake reflect related but non-identical biological processes. Reduced ADC is commonly associated with restricted water mobility and greater cellular density, whereas FDOPA uptake reflects amino acid transport and metabolically active tissue. These features may converge within aggressive viable tumor, yet necrosis, edema, microscopic infiltration, molecular subtype, partial-volume effects, and ROI selection can weaken their relationship. Prior voxel-wise and patient-wise analyses similarly found correlation between FDOPA PET and physiologic MRI parameters without complete biological equivalence [1]. Multimodal PET/MRI literature also supports complementary rather than interchangeable information from diffusion and metabolic imaging [4–6,11].

The pattern of grades made biological sense. PET activity rose from 25.0% in WHO grade 2 to 89.3% in grade 4 tumours, whereas mean ADC dropped and PET uptake increased with increasing grade categories. Studies with dynamic FDOPA have demonstrated additional value in identifying aggressive glioma behavior [8], and contemporary reviews support FDOPA for characterization and metabolic assessment [13]. Still, grade is not a complete description of glioma biology. The 2021 WHO framework requires integrated histological and molecular diagnosis, including markers such as IDH status and 1p/19q codeletion [14]. These variables were not sufficiently available for the present analysis.

The cohort-derived ADC threshold of ≤1.20 $\times 10^{-3}$ mm²/s produced high sensitivity but poor specificity. It identified most PET-active tumors, but 24 tumours that were not active on PET were found to be positive for ADC. The positive likelihood ratio that was found, 1.45, shows that the chance of PET-defined activity has only slightly increased. A stricter threshold made the accuracy better, but it missed a lot of active tumours. So, ADC can make you suspicious or help you get selective metabolic imaging, but it can't tell you on its own whether a tumour is metabolically active or inactive. The safest interpretation remains multimodal. Concordance of solid tumor morphology, FLAIR abnormality, diffusion restriction, contrast enhancement, susceptibility change, and amino acid uptake may identify clinically important tumor regions. Discord can also teach you something. A PET-active area with less restriction may still be alive and metabolically active, while a low-ADC area with little FDOPA uptake could be caused by cellular tissue, bleeding, technical issues, or differences in the samples used. This variety is the reason why a single ADC measurement can't be used instead of PET or a tissue-based diagnosis.

With a confidence level of 0.50, the AUC of 0.62 shows that the classification is weak and unclear. This finding is still useful because it makes it clear how much ADC can add when metabolic PET activity is used as the standard outcome. The results show that ADC should only play a supporting role in multimodal assessment [3–6,12,13].

LIMITATIONS

Based on a single institutional record, this study looked back at the past. Instead of taking direct histology samples of every metabolically active area, PET-defined metabolic activity was used as the standard result. Seven patients did not have available histopathology, but these cases were not included in grade-based studies.

It was not always possible to get back all of the technical information about the PET scan, such as the exact uptake interval, scanner model, reconstruction parameters, and carbidopa premedication status. These ideals were not put on someone. The exact time between the MRI and PET scan and the official state of blinding were also not known. MRI was done on a 1.5-T Philips platform, but not all examinations had full sequence-specific parameters available. Cases were given to four radiologists, but reader-level identifiers and independent measurements that were taken twice were not kept, so agreement between observers could not be checked.

The ADC threshold was selected and tested in the same cohort and may therefore overestimate performance. The 2-mm-diameter ROIs reduced contamination from obvious necrosis and lesion margins but sampled only small parts of heterogeneous tumors; they were also sensitive to pixel-level noise, placement variation, and partial-volume effects. The grade subgroups were relatively small, particularly WHO grade 3. Molecular annotation was incomplete, and no final multivariable prediction model was developed because of overfitting risk. The TBRmax threshold of 1.60 was an extrapolated baseline use of a PET RANO response-oriented rule and should not be interpreted as a universally validated FDOPA diagnostic or histological cutoff. Imaging-related adverse events were not systematically captured in the retrospective archive.

CONCLUSION

ADC showed a modest inverse relationship with ^{18}F-FDOPA uptake in this treatment-naïve cohort. PET-active tumors had lower mean ADC and higher SUVmax, but the groups overlapped substantially. The AUC was 0.62, and its lower confidence limit was close to chance-level discrimination.

The cohort-derived ADC level was very sensitive but not very specific, so it shouldn't be used as a sole clinical cutoff. At most, ADC can help with setting the scene of a multimodal review. It shouldn't be used by itself to choose people for PET, figure out metabolic activity, or plan treatment. Any clinical triage role needs to be approved by an outside group using standardized acquisition, molecular annotation, and repeatable ROI methods.

DECLARATIONS

Ethics Approval and Consent to Participate

The study was approved by the Medical Scientific Committee of Baghdad Teaching Hospital, Medical City, Baghdad, Iraq (approval no. 2-5543; 20 July 2026). The requirement for individual informed consent was waived because of the retrospective design and use of anonymized routine-care records.

Author Contributions

Imad Kh. Resen contributed to study conception, data organization, imaging-data review, statistical interpretation, manuscript drafting, critical revision, and approval of the final manuscript. The author accepts responsibility for the integrity of the work.

Conflict of Interest: The author reports no conflict of interest related to this work.

Funding: No external funding was reported for this study.

Data Availability: The de-identified data underlying the findings may be made available by the corresponding author upon reasonable request, subject to institutional and ethical approval.

Study Registration and Protocol: This retrospective study was not prospectively registered. A public study protocol was not available.

ACKNOWLEDGMENTS

The author thanks Dr Haider Nashmi, Jordanian Board-certified specialist in Diagnostic Radiology, for radiological consultation and methodological advice. The author also acknowledges the radiology and nuclear medicine staff of Baghdad Teaching Hospital, Medical City, for routine imaging acquisition and archival data retrieval.

REFERENCES

1. Tatekawa H, *et al.,* Voxelwise and patientwise correlation of ^{18}F-FDOPA PET, relative cerebral blood volume, and apparent diffusion coefficient in treatment-naïve diffuse gliomas with different molecular subtypes. J Nucl Med. 2021;62(3):319–325. doi:10.2967/jnumed.120.247411.
2. Kinoshita M, *et al.,* Magnetic resonance relaxometry for tumor cell density imaging for glioma: an exploratory study via ^{11}C-methionine PET and its validation via stereotactic tissue sampling. Cancers (Basel). 2021;13(16):4067. doi:10.3390/cancers13164067.
3. Jabeen S, *et al.,* Combined amino acid PET-MRI for identifying recurrence in post-treatment gliomas: together we grow. Eur J Hybrid Imaging. 2021; 5:15. doi:10.1186/s41824-021-00109-y.
4. Soni N, *et al.,* Amino acid tracer PET MRI in glioma management: what a neuroradiologist needs to know. AJNR Am J Neuroradiol. 2023;44(3):236–246. doi:10.3174/ajnr. A7762.
5. Harat M, *et al.,* Combining amino acid PET and MRI imaging increases accuracy to define malignant areas in adult glioma. Nat Commun. 2023; 14:4572. doi:10.1038/s41467-023-39731-8.
6. Langen KJ, *et al.,* Hybrid PET/MRI in cerebral glioma: current status and perspectives. Cancers (Basel). 2023;15(14):3577. doi:10.3390/cancers15143577.
7. Karlberg A, *et al.,* Diagnostic accuracy of anti-3-[^{18}F] FACBC PET/MRI in gliomas. Eur J Nucl Med Mol Imaging. 2024;51(2):496–509. doi:10.1007/s00259-023-06437-4.
8. Girard A, *et al.,* Additive value of dynamic FDOPA PET/CT for glioma grading. Front Med (Lausanne). 2021; 8:705996. doi:10.3389/fmed.2021.705996.
9. Nabavizadeh A, *et al.,* Distinguishing progression from pseudoprogression in glioblastoma using ^{18}F-fluciclovine PET. J Nucl Med. 2023;64(6):852–858. doi:10.2967/jnumed.122.264812.
10. Ouyang ZQ, *et al.,* Diagnostic accuracy of glioma pseudoprogression identification with positron emission tomography imaging: a systematic review and meta-analysis. Quant Imaging Med Surg. 2023;13(8):4943–4959. doi:10.21037/qims-22-1340.
11. Lohmeier J, *et al.,* Detection of recurrent high-grade glioma using microstructure characteristics of distinct metabolic compartments in a multimodal and integrative ^{18}F-FET PET/fast-DKI approach. Eur Radiol. 2024;34(4):2487–2499. doi:10.1007/s00330-023-10141-0.
12. Dadgar H, *et al.,* PET tracers in glioblastoma: toward neurotheranostics as an individualized medicine approach. Front Nucl Med. 2023; 3:1103262. doi:10.3389/fnume.2023.1103262.
13. Sipos D, *et al.,* Complex diagnostic challenges in glioblastoma: the role of ^{18}F-FDOPA PET imaging. Pharmaceuticals (Basel). 2024;17(9):1215. doi:10.3390/ph17091215.
14. Louis DN, *et al.,* The 2021 WHO Classification of Tumors of the Central Nervous System: a summary. Neuro Oncol. 2021;23(8):1231–1251. doi:10.1093/neuonc/noab106.
15. Bossuyt PM, *et al.,* STARD 2015: an updated list of essential items for reporting diagnostic accuracy studies. BMJ. 2015;351:h5527. doi:10.1136/bmj.h5527.
16. Albert NL, Galldiks N, Ellingson BM, van den Bent MJ, Chang SM, Cicone F, *et al.,* PET-based response assessment criteria for diffuse gliomas (PET RANO 1.0): a report of the RANO group. Lancet Oncol. 2024;25(1):e29–e41. doi:10.1016/S1470-2045(23)00525-9.
17. Stien G, Zinsz A, Ahrari S, *et al.,* PET-based response assessment criteria for diffuse gliomas (PET RANO 1.0): methodological application in [^{18}F]-FDOPA PET imaging. EJNMMI Res. 2025;15(1):44. doi:10.1186/s13550-025-01239-1.